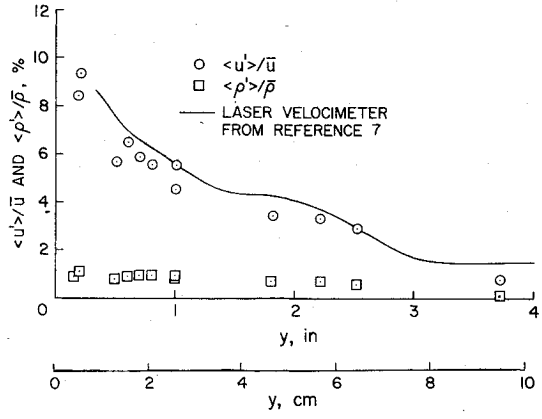

Fig. 3 Fluctuations of velocity and density through a $M_e = 0.8$ boundary layer.

Boundary-Layer-Turbulence Measurements

An application of the calibrations described in the preceding to measure the fluctuating velocity and density in a transonic boundary layer is discussed in the following. The boundary layer investigated was initially artificially thickened, and then allowed to develop on a flat-plate model in a $M = 0.8$ freestream flow in the Ames 6×6 ft wind tunnel. The characteristics of the boundary layer have been documented in Ref. 6, in which the model was denoted "configuration 5." The freestream unit Reynolds number was 4×10^6/ft (1.3×10^7/m), and the boundary-layer thickness was about 3.5 in. (9 cm); thus, $Re_\delta > 10^6$. The total temperature of the flow was near 530°R (295 K), and the surface of the flat-plate model was essentially adiabatic. The DISA model 55M constant-temperature system was used to drive the 5-μm tungsten wire, giving an upper frequency response in excess of 100 kHz for all flow conditions.

The fluctuating hot-wire data were reduced in the following manner. Since the total temperature fluctuations $T_t'/\bar{T}_t$ were everywhere less than about 0.3%,[6] the effect of these fluctuations on the wire's signal was neglected, and Eq. (5) was used to give $(\rho u)'/\bar{\rho}\bar{u}$. In order to separate $(\rho u)'$ into ρ' and u', an assumption about the fluctuating static pressure is required. Following the usual assumption of $p' = 0$, the technique of Kovasznay[2] can be used to obtain the following:

$$\frac{\langle u' \rangle}{\bar{u}} = \frac{1}{1 + (\gamma - 1)M^2} \frac{\langle (\rho u)' \rangle}{\bar{\rho}\bar{u}}$$

$$\frac{\langle \rho' \rangle}{\bar{\rho}} = \frac{(\gamma - 1)M^2}{1 + (\gamma - 1)M^2} \frac{\langle (\rho u)' \rangle}{\bar{\rho}\bar{u}}$$

The maximum uncertainties in the previous values for u' and ρ', due to the presence of pressure fluctuations, are given by plus or minus $\langle p' \rangle/\bar{p}$. The pressure fluctuations[6] for the present boundary layer are about 0.4% throughout the boundary layer. Thus, the values of $\langle u' \rangle/\bar{u}$ and $\langle \rho' \rangle/\bar{\rho}$, shown in Fig. 3 as a function of the distance across the boundary layer, could contain this ± 0.4% uncertainty. There are no direct measurements of the density fluctuations to compare with the present measurements. However, the observed density fluctuations appear to be reasonable when considering the mean gradient of density in this flow. For comparison, the velocity fluctuations obtained by Johnson and Rose,[7] using a laser velocimeter to study the same boundary layer, also are shown in Fig. 3. The agreement between these two independent measurement techniques gives credence to the hot-wire anemometer measurements and, in particular, to the calibrations and data-reduction procedures used here.

References

[1] Morkovin, M. W., "Fluctuations and Hot-Wire Anemometry in Compressible Fluids," AGARDograph 24, Nov. 1956.

[2] Kovasznay, L. S. G., "The Hot Wire Anemometer in Supersonic Flow," *Journal of the Aeronautical Sciences*, Vol. 17, Aug. 1950, pp. 565-572.

[3] Muhlstein, L., Jr., Petroff, D. N., and Jillie, D. W., "Experimental Evaluation of an Injector System for Powering a High Reynolds Number Transonic Wind Tunnel," AIAA Paper 74-632, July 1974.

[4] Rose, W. C., "The Behavior of a Compressible Turbulent Boundary Layer in a Shock-Wave-Induced Adverse Pressure Gradient," NASA TN D-7092, March 1973.

[5] Mateer, G. G., Brosh, A., and Viegas, J. R., "An Experimental and Numerical Investigation of Shock-Wave Turbulent Boundary-Layer Interaction at $M = 1.5$," AIAA Paper 76-161, Washington, D.C., Jan. 1976.

[6] Otten, L. J. III and Van Kuren, J. T., "Artificial Thickening of High Subsonic Boundary Layers," *AIAA Journal*, Vol. 14, Nov. 1976.

[7] Johnson, D. A. and Rose, W. C., "Turbulence Measurements in a Transonic Boundary Layer and Free-Shear Layer Flow Using Laser Velocimeter and Hot-Wire Anemometer Techniques," AIAA Paper 76-399, San Diego, Calif., June 1976.

Similarity in Vortex Asymmetries over Slender Bodies and Wings

Earl R. Keener* and Gary T. Chapman†
NASA Ames Research Center, Moffett Field, Calif.

Introduction

WHEN a body of revolution is pitched to high angles of attack at zero sideslip angle, a side force can occur. This asymmetric force is associated with the separation-induced vortex flowfield on the lee side of the body becoming asymmetric. At moderate angles of attack, the location of the flow separation and the resulting vortex flowfield are symmetric, but at high angles of attack, the flow separation and vortex flowfield can become asymmetric. When the flowfield is asymmetric, an asymmetric force (side force) can occur.

Because the configuration of the forebody plays an important role in the spin characteristics of aircraft, a comprehensive wind-tunnel test program was conducted at Ames Research Center in which static aerodynamic data were obtained for forebody-alone models. The tests covered a wide range of forebody shapes, Reynolds numbers, and Mach numbers.[1-6]

The results of these tests showed that the side forces are largest at subsonic speeds and that the magnitude of the side force can be larger than the maximum normal force. Furthermore, there was a well-defined angle of attack for the onset of side force; this onset angle varied only with forebody geometry and could be correlated with the semiapex angle of the nose by a simple formula: onset $\alpha = 2\delta_N$.

One consideration in the analysis of the experimental results was the cause of the vortex asymmetry, which is not understood completely. There are at least two possible causes for the flow becoming asymmetric: 1) a boundary-layer-induced asymmetry in the location of flow separation that causes the vortex flowfield to become asymmetric, or 2) a hydrodynamic (inviscid) instability in the pair of symmetrically separated vortices which causes the asymmetry.

Presented as Paper 76-66 at the AIAA 14th Aerospace Sciences Meeting, Jan. 26-28, 1976; submitted March 10, 1977; revision received June 20, 1977.

Index category: Aerodynamics.

*Research Scientist. Associate Fellow AIAA.

†Research Scientist, Chief, Aerodynamics Branch. Member AIAA.

This Note deals with the similarities between asymmetric flow about bodies and wings at high angles of attack. The analysis of the experimental results of the wind-tunnel test program yielded some evidence that the vortex asymmetry was the result of a hydrodynamic instability. In an effort to understand the cause of the asymmetry, additional examples of asymmetric flow were sought. Highly swept delta wings were one obvious possibility.

Effect of Fineness Ratio on Magnitude of Side Force

From the analysis of the side forces measured on various forebody models at high angles of attack and zero sideslip, it was found that forebody fineness ratio[1,3] has a large effect. This effect is shown in Fig. 1, in which data for forebody-alone models (no afterbody) having fineness ratios (length/maximum diameter) of $l/d = 2.5$, 3.5, and 5 are used. The test conditions are for a Mach number M of 0.25, a Reynolds number (R_d based on base diameter) of 0.8×10^6, and an angle of sideslip β of zero. The magnitude of the maximum measured side force coefficient C_Y is large for the $l/d = 3.5$ and 5 forebodies, but the maximum side force is nearly zero for the $l/d = 2.5$ forebody at the same Reynolds number. This effect of forebody fineness ratio also occurs for models with afterbody fineness ratios of $l/d = 7$, 9, and 11.[3] Thus, an onset of side force occurs as the forebody fineness ratio is increased above 2.5.

Consideration was given to a possible cause for this onset of side force with increasing nose fineness ratio. It was conjectured that decreasing the nose angle might cause the symmetric pair of vortices, which trail off the nose at high angles of attack, to be crowded together until the vortices become unstable; one vortex then gives way and slides up over the other, resulting in an asymmetric vortex flowfield and, consequently, an asymmetric aerodynamic force. If this is the case, it was speculated that a similar effect might occur with delta wings as the apex angle decreases. Consequently, existing reports on delta wing results were reviewed, and an excellent set of data by Shanks[7] was found. These data were obtained from tests of highly swept delta wings with semiapex angles of 6 to 20 deg, tested at high angles of attack (up to 40 deg) at low speed over a range of Reynolds numbers (R_l based on wing length) from 0.9×10^6 to 2.4×10^6. These data showed that, at angles of attack above 24 deg, a rolling moment occurred at zero sideslip for semiapex angles of less than 12 deg.

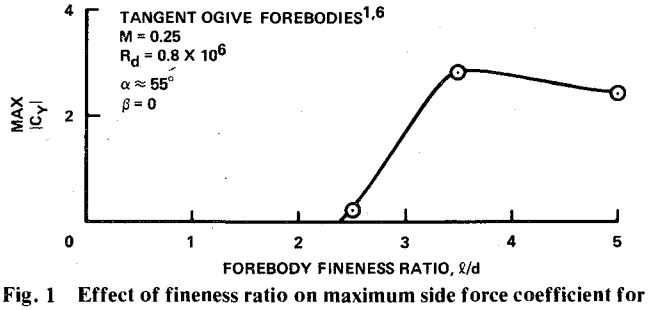

Fig. 1 Effect of fineness ratio on maximum side force coefficient for pointed tangent-ogive forebodies.

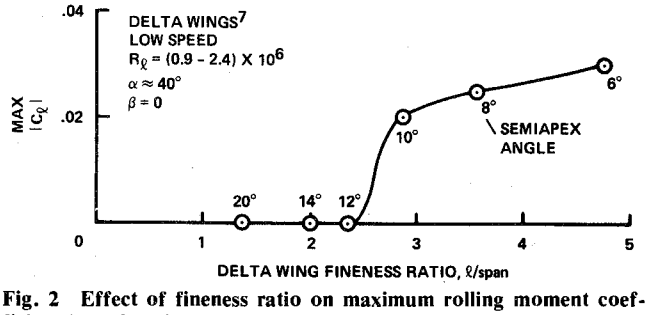

Fig. 2 Effect of fineness ratio on maximum rolling moment coefficient for delta wings.

To make them compatible with the data of Fig. 1, some of the data of Ref. 7 are plotted in Fig. 2 as maximum rolling-moment coefficient C_l vs wing fineness ratio (l/span); the semiapex angles also are shown. Note that the variation of wing rolling moment with wing fineness ratio in Fig. 2 is remarkably similar to the variation of side force with forebody fineness ratio in Fig. 1. Both wing rolling moments and body side forces are greatly affected by fineness ratio. These forces and moments are zero at fineness ratios of 2.5 and lower, but they become appreciable at fineness ratios greater than about 2.5 (wing semiapex angles less than 12 deg).

Because slender delta wings induce a pair of vortices by flow separation off the leading edge at moderate angles of attack, the occurrence of wing rolling moment at high angles of attack must result from an asymmetry in the wing vortex flowfield. The fact that similar asymmetries appear to occur in the flow over both forebodies and wings at high angles of attack suggests that the symmetric pair of vortices off the apex are crowded together as the slenderness increases (apex angle decreases) and that this crowding causes a hydrodynamic instability in the vortex flowfield and an asymmetry in the vortex formation. Note that for the swept wing the separation point is fixed at the leading edge, which implies that the asymmetry in separation point on a body of revolution is not necessarily an essential feature of vortex asymmetry.

Effect of Fineness Ratio on Angle of Onset

In Ref. 1, it was shown that the angle of attack at which onset of side force occurs also varies with forebody fineness ratio. The onset angle increases with decreasing forebody fineness ratio and can be correlated with a simple formula: onset $\alpha = 2\delta_N$, where δ_N is the semiapex angle of the nose. In Fig. 3, the angles of attack for the onset of rolling moment for the delta wings (determined from the data in Ref. 7) are compared to the curve for the onset angles for pointed forebodies as a function of semiapex angle. It was thought that the onset angles might correlate with $2\delta_N$ for bodies and delta wings; however, the onset angles for delta wings are appreciably higher than those for the forebodies at the same values of semiapex angle.

Concluding Remarks

It has been shown that, at high angles of attack and zero sideslip, an asymmetric moment (in roll) occurs on slender delta wings which is similar to the occurrence of an asymmetric force (side force) on slender circular forebodies. The similarity is demonstrated by the fact that both the forebody side force and the wing rolling moment occur as the fineness ratio is increased above about 2.5. The angles of attack of onset of these asymmetries increase as the apex angle is increased. Since the asymmetry in the forebody forces is known

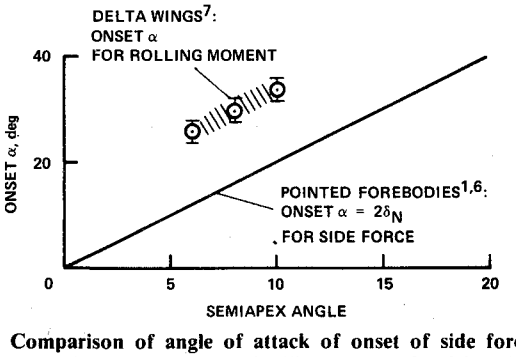

Fig. 3 Comparison of angle of attack of onset of side force for pointed forebodies to onset angle of rolling moment for delta wings.

to be associated with an asymmetry in the vortex flowfield on the lee side, the asymmetry in the wing rolling moments must be associated with a similar asymmetry in the wing vortex flowfield. The fact that the asymmetries occur as the slenderness is increased suggests that the cause of the vortex asymmetry is a hydrodynamic instability in the vortex flowfield resulting from the crowding together of the vortices as the apex angle is decreased. Furthermore, the fact that the separation point is fixed at the leading edge for delta wings implies that the asymmetry in separation point on a body of revolution is not necessarily an essential feature of vortex asymmetry.

References

[1]Keener, E.R. and Chapman, G.T., "Onset of Aerodynamic Side Forces at Zero Sideslip on Symmetric Forebodies at High Angles of Attack," AIAA Paper 74-770, 1974.

[2]Keener, E.R. and Taleghani, J., "Wind Tunnel Investigation of the Aerodynamic Characteristics of Five Forebody Models at High Angles of Attack at Mach Numbers from 0.25 to 2," NASA TM X-73,076, 1975.

[3]Keener, E.R., Chapman, G.T., and Kruse, R.L., "Effects of Mach Number and Afterbody Length on Onset of Asymmetric Forces on Bodies at Zero Sideslip and High Angle of Attack," AIAA Paper 76-66, Washington, D.C., Jan. 1976.

[4]Keener, E.R., Chapman, G.T., Cohen, L., and Taleghani, J., "Side Forces on a Tangent Ogive Forebody with a Fineness Ratio of 3.5 at High Angles of Attack and Mach Numbers from 0.1 to 0.7," NASA TM X-3437, 1976.

[5]Keener, E.R., Chapman, G.T., Cohen, L., and Taleghani, J., "Side Forces on Forebodies at High Angles of Attack and Mach Numbers from 0.1 to 0.7: Two Tangent Ogives, Paraboloid and Cone," NASA TM X-3438, 1976.

[6]Keener, E.R. and Valdez, J., "Side Forces on a Tangent Ogive Forebody with a Fineness Ratio of 2.5 at High Angle of Attack and Low Speed," NASA TM X-73, 176, 1976.

[7]Shanks, R.E., "Low-Subsonic Measurements of Static and Dynamic Stability Derivatives of Six Flat-Plate Wings Having Leading-Edge Sweep Angles of 70° to 84°," NASA TN D-1822, 1963.

A Model of Base Burning Propulsion Using Lateral Injection

D. W. Harvey* and Ivan Catton†
McDonnell Douglas Astronautics Company, Huntington Beach, Calif.

Nomenclature

A = area
L_c = cavity length
M = Mach number
$\dot{m}_i$ = injectant mass flow rate
P = pressure
U = velocity
δ = divergence angle of annulus
ρ = density
σ = mixing half-angle
θ_c = cone half-angle
θ_w = cavity half-angle

Subscripts

∞ = freestream
b = base

Received March 14, 1977; revision received June 3, 1977.
Index categories: Jets, Wakes, and Viscid-Inviscid Flow Interactions; Airbreathing Propulsion; Combustion and Combustor Designs.

*Senior Engineer/Scientist.
†Consultant; also Professor, Department of Energy and Kinetics, University of California, Los Angeles.

Introduction

THE use of fluid injection and combustion in the separated region behind blunt-based projectiles or vehicles has been a matter of interest ever since it became known that the base pressure could be raised by this means. Some of the early work is listed in Refs. 1-3. However, base pressures significantly above ambient values have proved difficult to reach, as can be seen by considering the most recent experimental program[4] in this area, in which base pressure ratios greater than 1 were obtained only at the cost of some questions of tunnel interference, and none greater than 2 were obtained at all.

Higher base pressure ratios may be accessible as a result of the concept developed by Strahle[2]; and other, more easily implemented methods of achieving high performance, such as the one discussed in this Note, may also exist.

Analysis

A model of base burning propulsion can be developed by modifying existing base flow methods to include the effects of injection. The Crocco-Lees and Korst-Chapman approaches have been the subjects of such modification,[5,6] but results have not been entirely satisfactory, due partly to the non-trivial problems involved in treating axial symmetry, and partly to the complexity of these methods, when regions of different fluids must be distinguished.

Another approach is to develop an analysis directly for the base burning case. This was done by Schetz et al. for base bleed only[7] and then extended to include lateral injection.[8] The model used accounts for many important features of the flow, including downstream mixing and coupling of the viscous wake flow with the inviscid surrounding flow. The model provides an interesting insight into the case of a high Mach number flow of low static temperature, but high stagnation temperature, when there is a question whether chemical reaction heats or cools the flow.

However, the model of Schetz et al. has limitations that make it less useful for lateral injection. As it stands, it does not treat the injection process in any detail. Further, in the near wake region, it appears to treat the cavity and the surrounding shear layer as a single one-dimensional (radially averaged) flow. Although this is a good assumption for massive base bleed, it is probably not as good for lateral injection.

The present work is an attempt to improve the treatment of lateral injection by using existing, detailed computer models of reactive liquid and gas injection (for the liquid injection case, see Ref. 9), combined into a code we refer to as BBLIP (for Base Burning/Lateral Injection Propulsion). In the component models, the injectant turns from its original direction and moves downstream in a central region surrounding by a shock layer. These regions are calculated stepwise downstream, with the central region expanding by mixing and combustion, and with pressure and direction equalized across the dividing streamline between the central region and the shock layer. Combustion is controlled by mixing for the case of a gas jet, and for a liquid jet by jet breakup, evaporation, and mixing.

At the base plane, the individual nozzle flows are transformed to a single annulus concentric with the body and axially symmetric, and the inner boundary of this annulus turns inward as shown in Fig. 1 to an angle θ_w. The inner boundary pressure presently is calculated using a simplified recirculation model, which includes a term accounting for the addition of base bleed, and thus allows evaluation of the possibly synergistic effect of combining base bleed and lateral injection. The outer boundary pressure is calculated from expansion of the outer flow through an angle $\theta_c + \theta_w - \delta$, where θ_c is the cone half-angle and δ is the divergence angle between inner and outer annulus boundaries. Note that because of axial symmetry, in general $\delta > 0$ even if the annulus flow is taken as frozen and without mixing. The streamwise